Viscous incompressible flow simulation using penalty finite element

R.L. SHARMA [1]
[1]Jawaharlal Nehru Government Engineering College
Sundernagar, Mandi, H.P.
INDIA
Emails: rls@nith.ac.in.

Abstract: - A new set of boundary conditions for velocity-divergence formulation of incompressible Navier–Stokes equations are derived. The boundary is characterized by traction due to friction and surface tension. The pressure being unknown is decoupled from the computation of velocity and is determined by post processing of the velocity field. Numerical results are presented for - classical lid-driven cavity flow- widely used by numerous authors due to its simple geometry and complicated flow behavior and squeezed flow between two parallel plates amenable to analytical solution and compared with benchmark and analytical results.

Key-Words: - Viscous incompressible flow; Finite elements, Penalty method, Boundary conditions; Surface traction

1 Introduction

The coupling of the velocity and pressure fields and correct implementation of pressure boundary conditions is the main problem in the numerical simulation of incompressible viscous flows. The real-life problems are usually three-dimensional which tremendously increase the computation load. Hence, efficient and accurate numerical methods are essential to the development of CFD techniques. The stream function–vorticity formulation [1] and [2], which eliminates pressure calculation, is well developed and established in two-dimensional incompressible flow analysis. However, the boundary condition for vorticity, especially on non-slip boundaries is difficult to be specified accurately and lead to error to the computation. On the other hand, the boundary conditions in primitive variables (velocity and pressure) formulation of the incompressible Navier–Stokes equations could be specified without further derivation. The accuracy of the various alternatives has been studied extensively in the literature. The finite element solution of the primitive variables formulation leads to a fully coupled matrix equation that provides accurate solution by solving both velocity and pressure implicitly. Cruchaga and Oñate [3] demonstrated a numerical solution by this approach. However, large computer resources are required to obtain the solution of the coupled formulation implicitly. Whereas, the additional computation load spends on solving fully coupled solution could be avoided by using velocity correction method [4] and [5], which decouples the velocity–pressure formulation and solves the primitive variables independently.

The velocity correction method (also called projection method) was discussed in detail in Gresho [6]. In another paper, Gresho and Chan [7] demonstrated the finite element solution of some viscous incompressible flow problems solved by the projection method of which the diffusion and convection terms are calculated implicitly and explicitly, respectively. This approach has the benefit of avoiding the non-linearity caused by the convection term which leads to the formation of a non-symmetric coefficient matrix and instabilities in convection dominated flow. Moreover, the negative numerical diffusivity caused by solving the convection term explicitly is compensated by using a balancing diffusion tensor [7].

The present study generally follows a similar approach and uses penalty finite element method to decouple the incompressible Navier–Stokes equation. This method seeks to eliminate the continuity equation to get rid of pressure - the most unusual quantity in the N-S equations. It is subsequently determined from the velocity at time ‘t’ without any time lag. Unlike the finite difference method and the spectral method, the finite element method is convenient for handling arbitrarily shaped domains and variable resolution meshes [3]. The adopted mathematical model and its implementation is discussed in detail in the following sections.

The accuracy of the solution, however, involves specification of the proper boundary conditions [6-7]. Using penalty method neither the pressure nor its normal gradient on the boundaries are known until the velocity field is determined. Prescription of any

ISBN: 978-960-474-376-6

erroneous boundary stresses may result in distortion of solution in the interior of the domain. Peyret and Taylor [8], in their book on computational fluid mechanics, also identify the specification of correct pressure boundary conditions as the primary difficulty.

In this paper we replace the pressure boundary conditions by gradient of velocity to avoid distortion of solution and employ fully discrete approximation procedure for the solution of transient Navier-Stokes equations based on Crank Noclson scheme in time and finite element method in space. It is then applied to classical lid-driven square cavity flow and squeezing flow between parallel plates. The results are compared with benchmark results published in the literature

2 Governing Equations

The governing equations for isothermal, viscous incompressible flow over a domain enclosed by the boundary $\partial\Omega = \Gamma_1 \cup \Gamma_2$ are:

$$\frac{\partial \mathbf{u}}{\partial t} + (\mathbf{u} \cdot \nabla)\mathbf{u} = -\nabla p + \frac{1}{\mathrm{Re}} \nabla^2 \mathbf{u} + f \quad in \quad \Omega \quad (1)$$

$$div\ \mathbf{u} = 0 \qquad in \qquad \Omega \quad (2)$$

Where u is the velocity vector, p is the kinematic pressure (pressure divided by constant density), Re is Reynolds number which is reciprocal of the kinematic viscosity, f is body force vector and t is the time. The effect of stresses in Eq. (1) is represented by and terms, which are gradients of surface forces, analogous to stresses in solids. The term is pressure gradient and arises from normal stresses that turn up in almost all situations and conventionally represents the shear effect for incompressible flow.

The equation (1) comprises of time-dependent system of nonlinear partial differential equations in primitive variables. It can be viewed as the respective equations for the velocity components, implying that the divergence-free condition (2) must be solved for pressure which is particularly difficult because the pressure does not appear explicitly in this equation. Presence of non-linear, non-symmetric convective terms in equation (1) presents another difficulty particularly at high Reynolds number flows which are convection dominated. Equation (2) is more specifically a statement of the conservation of mass. Together, the set of equations (1) and (2) represent a constrained coupled problem. Any numerical solution to N-S equations (1) apart from verifying the dynamic constitutive equation has to satisfy in addition the incompressibility condition (2).

3 Boundary Conditions

For conciseness, we breakup into two subsets: and, over which displacements and stresses, respectively are specified. Two transitional relations are to be satisfied for fluid at a material boundary i.e. continuity of intensity across the surface and the continuity of normal component of flux vector. For viscous incompressible flow, momentum is the transportable quantity across the interface; hence, specifications of boundary conditions at a surface involve continuity of velocity and continuity of stress.

3.1 Continuity of Velocity

In case of viscous flow the boundary conditions for $\partial\Omega = \Gamma_1$ i.e. on solid walls, the velocity must satisfy both no-slip and no-flux conditions. No slip condition requires that the tangential component of the fluid velocity be the same as the tangential component of the velocity of the surface i.e.

$$\mathbf{u}.\mathbf{t} = \bar{\mathbf{u}}.\mathbf{t} \quad (3)$$

Where, $\bar{\mathbf{u}}$ is a given function describing the velocity of the boundary Γ_1 and t is a unit vector tangent to the boundary. This condition is used almost universally in modeling of viscous flows and is essentially a conservation of tangential velocity; if the boundary is stationary, $\bar{\mathbf{u}}.\mathbf{t} = 0$ and by equation (3) above we have, $\mathbf{u}.\mathbf{t} = 0$ giving $u = v = 0$. Similarly, no-flux condition requires that the normal component of the velocity of the fluid must be same as the normal component of the velocity of the boundary i.e.

$$\mathbf{u}.\mathbf{n} = \bar{\mathbf{u}}.\mathbf{n} \quad (4)$$

Where, **n** denotes the outward pointing normal on Γ. If this were not being the case, the resulting discontinuity would essentially be a rupture or shock in the medium and we have not assumed any event that would cause such a phenomena. Further, any discontinuity across a boundary would result either in a transport of the differences of fluid across the boundary, which would not then be impermeable, or there would be an unbounded positive or negative accumulation of fluid by the wall. Boundary condition (4) is known as no flux or

ISBN: 978-960-474-376-6

no penetration condition. Combining Eq. (3) and (4) we have

$$\mathbf{u} = g_1 \quad \text{on} \quad \Gamma_1 \qquad (5)$$

The boundary conditions (5) imply that the fluid velocity must match the velocity of the rigid boundary at every point on it. It represents essential or Dirichlet boundary conditions which assign values to dependant variables. It is obtained from kinematic considerations - a condition which relates the motion of the boundary to the fluid velocities and is applicable on rigid and symmetry planes of the boundary Γ_1.

3.2 Continuity of Stress

Boundary tractions and contact forces (because of friction and surface tension) acting on Γ2 lead to pressure or stress boundary conditions. Considering a small area dA bounded by a closed contour C and characterized by surface traction tn and surface tension γ, the net force on the element dA is given by

$$\mathbf{f}_s = \int_S \mathbf{t}_n \, dA + \int_C \gamma \, dl \qquad (6)$$

Where, dl is small length along the curve C. Although the forces in the conservation of linear momentum equation may be left in terms of surface tractions, it is more convenient and customary to put the stress vector $\mathbf{t}_n$ in terms of stresses on the planes perpendicular to the coordinate axes, i.e. in terms of the components of the stress as

$$\mathbf{t}_n = \mathbf{n} . \mathbf{T} \qquad (7)$$

Where, $\mathbf{T}$ is Cauchy stress tensor (normalized by density). The elements of $\mathbf{T}$ are associated with normal and tangential forces and can be expressed as the sum of mean hydrostatic stress tensor, pI which tends to change the volume of the fluid element; and deviatoric stress as

$$\mathbf{T} = -p\mathbf{I} + \nu \left(\nabla \mathbf{u} + (\nabla \mathbf{u})^T \right) \qquad (8)$$

Where, I is the identity tensor. The part $-p\mathbf{I}$ represents the stresses due to compression of the fluid. The part $\nu \left(\nabla \mathbf{u} + (\nabla \mathbf{u})^T \right)$ represents viscous stress tensor which tends to distort the body and depend on the velocity of the fluid. It gives the force in a direction parallel to the surface. Substituting the expression for stress tensor in (7) and integrating, we have

$$\int_S t_n \, dA = \int_S \left\{ -p\mathbf{I} + \nu \left(\nabla u + (\nabla u)^T \right) \right\} . \mathbf{n} \, dA \qquad (9)$$

Also form Stokes theorem, we have

$$\int_C \gamma \, dl = \int_S \left[-\gamma \mathbf{n} \left(\nabla^s . \mathbf{n} \right) + \nabla^s \gamma \right] dA \qquad (10)$$

Where, $\nabla^s = \nabla - \mathbf{n} \left(\mathbf{n} . \nabla \right)$ is the component of gradient operator in the local plane of the interface. $\nabla^s . \mathbf{n}$ is the mean curvature of the interface which can be expressed as the sum of two radii of curvature R1 and R2 of the interface in any two orthogonal planes as $\nabla^s . \mathbf{n} = \frac{1}{2} \left(\frac{1}{R_1} + \frac{1}{R_2} \right)$. On the right hand side (Eq. 10), $\gamma \mathbf{n} \left(\nabla^s . \mathbf{n} \right)$ is the normal curvature force per unit area and $\left(\nabla^s \gamma \right)$ is the tangential stress associated with gradient of surface tension, both of which will vanish, if either the curvature of the interface or the surface tension vanishes. Using equations (9 -10), the surface force fs become

$$f_s = \int_S \left\{ -p\mathbf{I} + \nu \left(\nabla \mathbf{u} + (\nabla \mathbf{u})^T \right) \right\} . \mathbf{n} \, dA + \int_S \left[-\gamma \mathbf{n} \left(\nabla^s . \mathbf{n} \right) + \nabla^s \gamma \right] dA \qquad (11)$$

Since dA is arbitrary, the integrand must vanish identically giving

$$\boldsymbol{\sigma} = -p . \mathbf{n} + \nu \left(\nabla \mathbf{u} + (\nabla \mathbf{u})^T \right) . \mathbf{n} - \gamma \mathbf{n} \left(\nabla^s . \mathbf{n} \right) + \left(\nabla^s \gamma \right) \quad \text{on} \quad \Gamma_2 \qquad (12)$$

Where, σ is the total stress vector acting on a plane perpendicular to the coordinate axis having the unit normal n. It serves as a traction boundary condition at the free surface, typically complementing the Navier-Stokes equations at the far field. The stress vector σ may not necessarily be perpendicular to the plane, i.e. parallel to n, and can be resolved into scalar components i.e. normal and tangential (shear traction).

3.3 Normal Stress

The normal stress component, σn of any stress vector in terms of the component of the stress tensor is the dot product of the stress vector and the unit vector n normal to the surface, thus

$$\boldsymbol{\sigma}_n = \boldsymbol{\sigma} \mathbf{n} \qquad (13)$$

Using equation (13), we have

$$\boldsymbol{\sigma}_n = \left[-p . \mathbf{n} + \nu \left(\nabla \mathbf{u} + (\nabla \mathbf{u})^T \right) . \mathbf{n} - \gamma \mathbf{n} \left(\nabla^s . \mathbf{n} \right) + \left(\nabla^s \gamma \right) \right] . \mathbf{n}$$

$$= -p \left(\mathbf{n} . \mathbf{n} \right) + \nu \left(\nabla \mathbf{u} + (\nabla \mathbf{u})^T \right) \left(\mathbf{n} . \mathbf{n} \right) - \gamma \left(\nabla^s . \mathbf{n} \right) \left(\mathbf{n} . \mathbf{n} \right) + \left(\nabla^s \gamma \right) . \mathbf{n}$$

ISBN: 978-960-474-376-6

$$= -p + \nu\left(\nabla \mathbf{u} + (\nabla \mathbf{u})^T\right) - \gamma\left(\nabla^S . \mathbf{n}\right) + \left(\nabla^S \gamma\right). \mathbf{n}$$
$$= -p + \nu \nabla \mathbf{u}.\mathbf{n} - \gamma\left(\nabla^S . \mathbf{n}\right) + \left(\nabla^S \gamma\right).\mathbf{n} ,$$
Since $\nabla \mathbf{u} = (\nabla \mathbf{u})^T$ (14)

Noting that $\left(\nabla^S \gamma\right). \mathbf{n} = 0$ since is tangent to the surface, the normal boundary condition (14) can be written as

$$-p + \nu \nabla u.\mathbf{n} - \gamma\left(\nabla^S . \mathbf{n}\right) = g_2 \text{ on } \Gamma 2 \quad (15)$$

This condition indicates that the interface curvature times the surface tension and pressure must balance the given normal stress. In the case where Γ_2 is a planer surface, $\nabla^s.\mathbf{n} = 0$, the equation (15) reduces to

$$-p + \nu \nabla u.\mathbf{n} = g_2 \quad \text{on } \Gamma_2 \quad (16)$$

3.4 Tangential Stress

The tangential stress component, σt of any stress vector σ in terms of the component of the stress tensor is given by

$$\sigma_t = \sigma.t \quad (17)$$

Where, t is a unit tangential vector. Using (12), we have

$$\sigma_t = \left[-p\,\mathbf{n} + \nu \mathbf{n}\left(\nabla \mathbf{u} + (\nabla \mathbf{u})^T\right) - \gamma \mathbf{n}\left(\nabla^s . \mathbf{n}\right) + \left(\nabla^s \gamma\right)\right]. \mathbf{t}$$
$$= -p\,(\mathbf{n}.\mathbf{t}) + \nu\left(\nabla \mathbf{u} + (\nabla \mathbf{u})^T\right)(\mathbf{n}.\mathbf{t}) - \gamma\left(\nabla^s . \mathbf{n}\right)(\mathbf{n}.\mathbf{t}) + \left(\nabla^s \gamma\right).\mathbf{t}$$
$$= \nabla^s \gamma \quad in \quad \Gamma_2 \quad (18)$$

Which, indicates that the tangential stress at a surface must be balanced by the gradient of local surface tension. The effect of surface tension applies only in the normal direction since the attractive forces on the molecules between the two mediums will always apply in the direction normal to the fluid interface. Since no such difference in potential forces exists in the tangential direction, equation (18) reduces to

$$\sigma_t = 0 \quad \text{on } \Gamma_2 \quad (19)$$

In fact, for incompressible flows, no boundary conditions for pressure are necessary. It is closely related to continuity equation and when the continuity equation is dropped or eliminated, the pressure term will also disappear as is shown later.

In case of time dependant problems, the fluid is also assumed to satisfy the initial condition

$$\mathbf{u}_{|t=0} = \mathbf{u}_0 \quad in \quad \Omega \quad (20)$$

This condition is used to define the initial state of the domain Ω. However, the initial velocity field must be solenoidal, i.e. $\nabla.\mathbf{u}_0 = 0$. A typical divergence free condition correspond to a stationary flow is u0 = 0. For pressure, no initial conditions need to be specified as no time derivatives of pressure appear in the governing equations. Thus we have the boundary conditions

$$\mathbf{u} = g_1 \quad \text{on} \quad \Gamma_1 , \quad (21)$$
on Γ2 and
$$-p + \nu \nabla u.\mathbf{n} = g_2 ; \quad \sigma_t = 0 \quad (22)$$

$$\mathbf{u}_{|t=0} = \mathbf{u}_0 \quad in \quad \Omega \quad (23)$$

Which together with governing equations (1-2) completely specify the problem.

4 Mathematical Formulations

In penalty function formulation [5], the continuity equation (2) is modified by adding a small term containing pressure as

$$P/\lambda + div\,\mathbf{u} = 0 \quad (24)$$

Giving, $P = -\lambda\, div\,\mathbf{u}$ (26)

Where, $\lambda = \mathrm{Re}\ \mu\ \beta$ is penalty parameter, Re and μ are respectively the Reynolds number and viscosity of the fluid and β is arbitrary large number, say, 10^7 *to* 10^{10} in double precision calculations.. The added term introduces damping to the continuity equation, reduces the divergence and help in recovering the incompressibility quickly. Eliminating the pressure P the governing flow equation (1) results in

$$\frac{\partial \mathbf{u}}{\partial t} + (\mathbf{u}.\nabla)\mathbf{u} - \frac{1}{\mathrm{Re}} \nabla^2 \mathbf{u} - \lambda \nabla(div\,\mathbf{u}) = f \quad (27)$$

Strict compliance of incompressibility constraint (Eq. 2) is abandoned in view introduction of penalized term in the momentum equation; thus eliminating the issue of a pressure boundary condition associated with the original primitive variable formulation.

ISBN: 978-960-474-376-6

The standard weak form is obtained by the application of weighted residual method i.e. by decretizing the equation (27), multiplying it by an arbitrary test function w and integrating, we have

$$\int_{\Omega}\left[\frac{\partial \mathbf{u}}{\partial t}+(\mathbf{u}.\nabla)\mathrm{u}-\frac{1}{\mathrm{Re}}\nabla^{2}\mathrm{u}-\lambda\nabla(\nabla.\mathbf{u})\right]w\,d\Omega=\int_{\Omega}\mathbf{f}\,w\,d\Omega \quad (28)$$

Integrating equation (28) and using the relations

$$\mathrm{w}\,\nabla^{2}\mathrm{u} = \mathrm{div}(\mathrm{w}\,\nabla\mathrm{u})-\nabla\mathrm{w}.\nabla\mathrm{u},$$

$$\mathrm{w}\,\nabla(\nabla.\mathbf{u}) = \frac{\partial}{\partial \mathrm{x}}(\mathrm{w}\,\nabla\mathrm{u})-\nabla\mathrm{w}.\nabla\mathrm{u}$$

together with Gauss divergence theorem $\int_{\Omega}\mathrm{div}\,\mathbf{a}\,d\Omega=\int_{\Gamma}\mathbf{a}.\mathbf{n}\,d\Gamma$, with n as outward normal and choosing, a = we obtain the weak form

$$\int_{\Omega}\left[\frac{\partial \mathbf{u}}{\partial \mathrm{t}}\mathrm{w}+\mathrm{w}(\mathbf{u}.\nabla)\mathbf{u}+\frac{1}{\mathrm{Re}}(\nabla\mathrm{w}.\nabla\mathrm{u})+\lambda(\nabla\mathrm{w}.\nabla\mathrm{u})\right]d\Omega$$
$$=\int_{\Omega}f\;w\,d\Omega+\frac{1}{\mathrm{Re}}\int_{\Gamma}w\nabla\mathrm{u}.\mathbf{n}\;d\Gamma+\lambda\int_{\Gamma}w\nabla\mathrm{u}.\mathbf{n}\;d\Gamma$$

(29)

Once the elementary matrices are evaluated and assembled, the Eq. (29) can be expressed as

$$[M]\left\{\dot{\mathbf{u}}\right\}+[K+K^{\lambda}]\{\mathbf{u}\}=\{F\} \quad (30)$$

Where M is the standard mass matrix, K is viscosity matrix arising from viscous terms and is so called penalty matrix having the same structure as K. The term F represent aggregate force produced by body forces and stresses (normal and tangential) acting on the surface. It may be observed that matrices K and are proportional to and respectively. In order to impose compressibility constraint, the parameter must be selected sufficiently large so that it plays a significant role to yield correct results. If is too small, compressibility and pressure errors will result and if too large it may result in numerical ill conditioning. Indeed, computations with this approach show that the velocity behaves rather well, but the pressure produces unrealistic wiggles (Sani et al 1981). These wiggles have been avoided by resorting to selective reduced integration.

Crank-Nicolson scheme [7], with step size$\Delta t = 0.1$, has been used to reduce the parabolic equation (30) to ordinary differential equations. The scheme is unconditionally stable, even though it is slightly more complicated and computationally intensive. The ordinary differential equations are then solved using Gauss elimination scheme iteratively starting with pseudo solution u0 satisfying the divergence-free condition (2). After each time step, the pseudo solution uj is made equal to the computed solution at the previous time level. To obtain steady state solution, the process was continued until the difference of velocity between two consecutive time steps becomes negligibly small i.e. $\left|u^{j}-u^{j-1}\right|\le\varepsilon_{\max}$.

5 Results and Discussions

The performance of the above mentioned numerical model was tested with two common flow cases: lid-driven cavity flow squeezing flow between parallel plates.

5.1 Lid-driven cavity

The first case is the classical lid-driven cavity flow which is commonly adopted for validating newly developed CFD models. Due to its simple geometry and complicated flow behavior, it has been widely used by numerous authors viz. Ghia et al. [1], Burgraff [9], Young and Lin [10], Botella and Peyret [11], Eldho and Young [12], etc. Fig. 1 shows the geometry of the computational domain and the adopted boundary conditions. The two-dimensional domain is a square cavity of width H that is fixed with three stationary and impermeable walls. The flow inside the cavity is driven by the upper sliding fluid moving with constant velocity Uref. The flows at the two upper corners are set to zero velocity and the first nodes from the corners are set to Uref/2. The Reynolds number Re is based on the reference velocity Uref and the reference length scale H (i.e., Re = UrefH/ν).

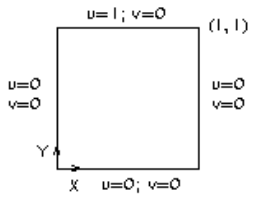

Fig. 1: Geometry and Boundary Conditions for the Square Cavity

ISBN: 978-960-474-376-6

Numerical results for different Reynolds numbers were obtained by adjusting the kinematic viscosity (ν) while the reference velocity and length scales were fixed. In the present study 64×64 and 128×128 grid system were used for Re□400 and Re = 1000, respectively. A converged solution for Re =1.0 (not shown here) with an assumption of u0 = v0 = 0 was obtained, which was then used as the initial guess for the case of Re =100, and so forth. For the comparison with other published results, the length scale is normalized by H while the computed velocity and pressure are normalized by Uref and Uref2, respectively.

Fig. 2 shows the computed results with Re = 10, 100, 1000 and 5000 along the horizontal and vertical lines passing through the geometric center of the cavity. For comparison, the computed results of Ghia et al. [1] are also shown. Good agreements between the two computations for both streamwise and spanwise velocity profiles are obtained that ensure the accuracy of the adopted method.

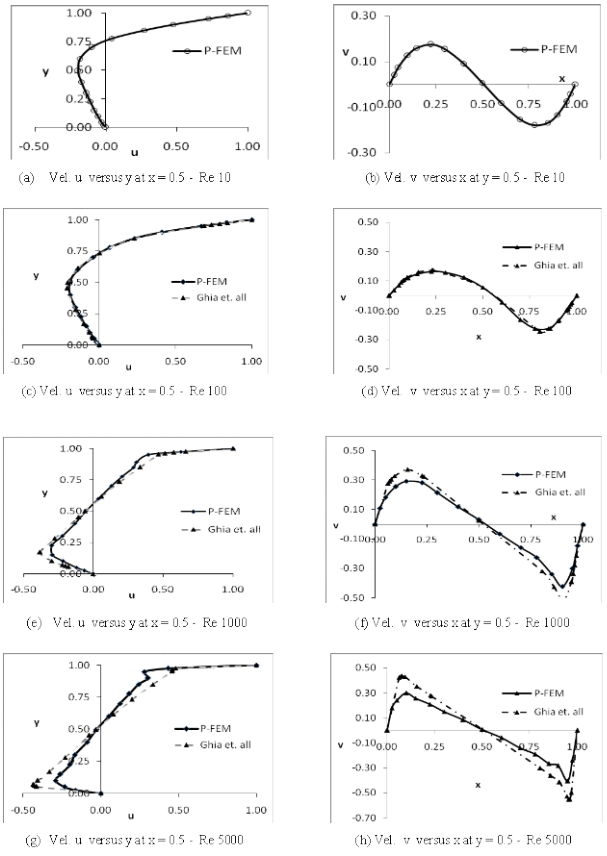

Fig. 2: Velocity profiles along central horizontal and vertical line of the cavity

The magnitudes of maxima and minima of both velocity profiles is also indicated in Table 1. The minimum of u along the center of the vertical line at x = 0.5 is denoted by umin. Similarly maximum and minimum of v along the horizontal line at y = 0.5 are denoted by vmax and v min respectively. The results show that the locations of these maxima move towards the stationary walls of the cavity as the Reynolds number increases.

Table 1: Characteristic values of the solution extrema on the horizontal and vertical line through center of the cavity

Re	*P-FEM Solution*				*Ref. (20) Solution*			
	u_{min}	v_{max}	v_{min}	J	u_{min}	v_{max}	v_{min}	J
10	-0.1950	0.1736	-.01803	186	-	-	-	-
100	-0.1921	0.1647	-0.2243	213	-0.2058	0.1750	-0.2453	-
1000	-0.2973	0.2910	-0.4240	839	-0.3828	0.3709	-0.5155	-
5000	-0.2912	0.2991	-0.4066	7500	-0.4364	0.4364	-0.5540	-

Though the results are obtained for Reynolds numbers as high as 5000, however, it can be noticed that as the Reynolds number increases, the convergence becomes slow owing to the diminishing thickness of the viscous layer, thus increasing the number of iterations required to attain the same degree of accuracy (εmax =1.0 x 10-6). This behavior is evident from Table (1) where, results for velocity along the vertical line through the center of the cavity are given.

The pressure was computed once the velocity profile was obtained. The pressure variation along the horizontal and vertical lines through the cavity center is shown in figure 3 for Re = 100, 1000 and 5000. The solution in this case can be expected to be of good accuracy.

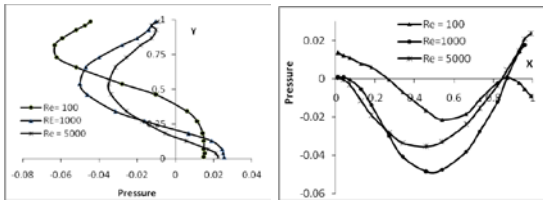

Fig. 3: Pressure profiles along central vertical and horizontal lines of the cavity

The comparison of pressure variation is also made with the model results of Botella and Peyret [13] for Re = 1000, wherein, the results of pressure field are given after setting the pressure equal to zero at the center (0.5, 0.5) of the cavity. Therefore, for the sake of comparison, free scale factor is chosen to make the pressure zero at the center of the cavity. The comparison is shown in figure 4 at Re =

ISBN: 978-960-474-376-6

1000. The agreement is seen to be good with the model results. As is obvious from the figures, the small difference near the ends is caused by effect of element division in the present investigation. However, both the results show a similar tendency, thus verifying the validity of the method.

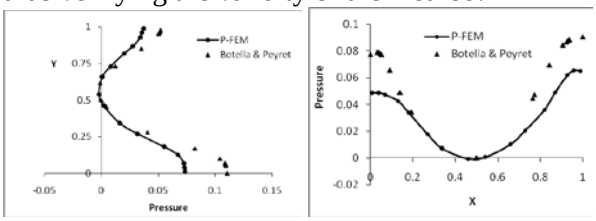

Fig. 4: Comparison of pressure profiles along central vertical and horizontal lines of the cavity

5.2 Squeezing flow between parallel plates

The second problem considered to test the capability of the present model for handling both the Dirichlet and Neumann boundary conditions is the squeezed flow between two parallel plates. The plates are assumed to be moving symmetrically about the line of axial symmetry towards each other at a constant velocity, v0 = 1. This would impart momentum to the fluid and would set up a velocity gradient in the fluid.

Figure 5 shows a schematic of computational domain and the dimensions for the two dimensional fully developed flow. The outflow boundaries are located at x = ± L. The plates are considered long enough for the velocity profile to become invariants at the exit plane

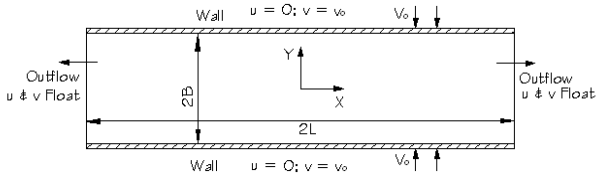

Fig. 5: Dimensions of the Modeling Region and Boundary Conditions

At the moving walls, $y = \pm$ B the Dirichlet boundary condition 22 will be applicable i.e.

$$u = 0 \text{ and } v = v_0 \quad \text{on} \quad \Gamma_1 \qquad (31)$$

The outer boundaries are chosen to be far enough so that the flow at the exit planes is fully developed. No traction boundary conditions at these planes follow from equation 22 which is:

$$-p.n + \nabla u.n = 0 \quad on \quad \Gamma_2 \qquad (32)$$

The problem is also transient in nature and has to be solved with appropriate initial conditions which has been taken as

$$u = 0 \quad \text{at} \quad t = 0 \quad \text{in} \quad \Omega \qquad (33)$$

The two dimensional analysis are performed with fluid parameters and Reynolds number $R_e = 1$. The instantaneous velocity field is obtained by solving the Eq. (1) together with boundary conditions for this geometry. The results are shown in Figures 6 and 7. Figures 6a shows the variation of velocity u with y at x = 6, whereas, Figure 6b shows the variation of velocity component v with y. Clearly the velocity v varies from -1.0 at the boundary to zero at the center as anticipated. The comparison of computed velocity profiles with the approximate analytical solution of Nadai [13] shows an excellent agreement between the two.

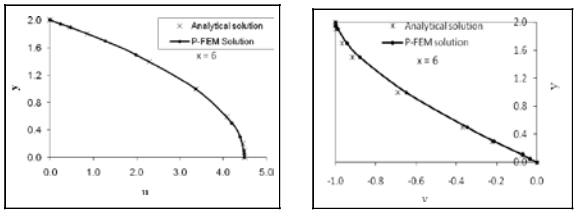

Fig. 6: Comparison of computed velocity profiles with analytical solution

The pressure has been calculated by post-processing the velocity field using $P = -\lambda(\nabla.u)$. The variation of pressure along the length of plate has been plotted at $y = \pm y_0$, where y0 is the y -coordinate of the Gauss point. Figure 7a shows the plot of pressure variation at $x = \pm 0.02$ $y = \pm 0.02$ along the length of the plate, whereas, figure 7b shows the pressure variation across the gap between the plates at . The pressure at the walls is marginally higher than that in the central core. These figures indicate that in this case both $\partial P / \partial x$ as $\partial P / \partial y$ are non zero.

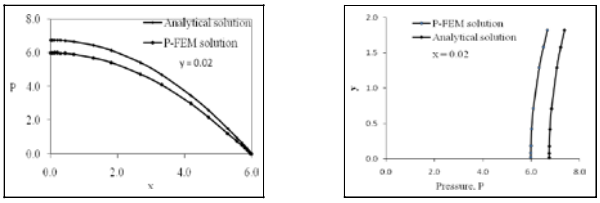

Fig.7: Comparison of computed pressure profiles with analytical solution.

6 Conclusions

We present the successful application of penalty finite element method to viscous incompressible flow problems governed by Navier - Stokes equations. The penalty variational formulation using finite element approximation has been constructed and discussed. The solution requires specification of boundary conditions about the velocity field and its velocity gradients at the natural boundaries of the flow domain. Formulation of such boundary conditions on synthetic boundary characterized by traction due to friction and surface tension has been discussed and investigated in greater detail.

The present numerical model was validated with two flow cases: flow inside a driven cavity and squeezing flow between two parallel plates. The calculated results compared well with benchmark numerical and analytical results. With good agreement between the two, it is concluded that penalty finite element method is a convenient way to satisfy the incompressibility constraint and to eliminate the pressure as an unknown from the formulation, thus reducing the number of degrees of freedom in the discretization. It can be successfully applied to solve incompressible viscous as well as inviscid fluid problems over a wide range of Reynolds numbers. However, as the Reynolds number increase, the convergence become slow and need more iterations to acquire the same degree of accuracy.

References:

[1] U. Ghia, K.N. Ghia and C.T. Shin, High-Re solutions for incompressible flow using the Navier-Stokes equations and a multigrid Method, Jr. Comp. Physics, 48, 387- 411, 1982.Eer

[2] G. Comini, M. Manzan and C. Nonino, Finite element solution of the stream function – vorticity equations for incompressible two-dimensional flows. Int. J. Num. Meth. Fluids, 19, pp. 513–525, 1994.

[3] M.A. Cruchaga and E. Oñate, A finite element formulation for incompressible flow problems using a generalized streamline operator. Comp. Methods Appl. Mech. Engrg., 143, pp. 49–67, 1997.

[4] A. Kovacs and M. Kawahara, A finite element scheme based on the velocity correction method for the solution of the time-dependent incompressible Navier–Stokes equations. Int. J. Num. Meth. Fluids, 13, pp. 403–423, 1991.

[5] G. Ren and T. Utnes, A finite element solution of the time-dependent incompressible Navier–Stokes equations using a modified velocity correction method. Int. J. Num. Methods Fluids, 17, pp. 349–364, 1993.

[6] P. M. Gresho and R. L. Sani, On the pressure boundary conditions for the incompressible Navier–Stokes equations, Int. J. Num. Meth. Fluids, Vol. 7, pp 1111, 1987.

[7] P.M. Gresho and S.T. Chan, On the theory of semi-implicit projection methods for viscous incompressible flow and its implementation via a finite element method that also introduces a nearly consistent mass matrix. Part 2: Implementation. Int. J. Num. Methods Fluids, 11 (1990), pp. 621–659, 1990.

[8] R. Peyret and T. D. Taylor, Computational Method for Fluid Flow, Springer-Verlog Berlin, 1983.

[9] O.R. Burggraf, Analytical and Numerical Studies of the Structure of Steady Separated Flows, Jr. Fluid Mechanics, Part 1, 113-151, 1966.

[10] D.L. Young and Q.H. Lin, Application of Finite Element Method to 2-D Flows, Proc. 3rd Nat. Con. Hydraulic Eng., Taipei, 223-242, 1986.

[11] O. Botella and R. Peyret, Benchmark Spectral Results on the Lid-Driven Cavity Flow, Comp. & Fluids, 27, 421-433, 1998.

[12] T.L. Eldho and D.L. Young, Two Dimensional Incompressible Viscous Flow Simulation Using Velocity-Vorticity Duel Reciprocity Boundary Element Method, Jr. Mechanics, Vol. 20, pp 177-185, 2004.

[13] A. Nadai, Theory of flow and fracture of solids, Vol. II, McGraw-Hill, New York, 1963.